MJFAS
Malaysian Journal of Fundamental and Applied Sciences

Rusydi *et al.* | Malaysian Journal of Fundamental and Applied Sciences, Vol. 20 (2024) 1136-1148

RESEARCH ARTICLE

Electronegativity Effects on Conformational Stability Using Bent's Rule: From Simple Molecules to Acetylcholine

Febdian Rusydi[a,b*]

[a]Department of Physics, Faculty of Science and Technology, Universitas Airlangga, Surabaya 60115, Indonesia; [b]Research Center for Quantum Engineering Design, Faculty of Science and Technology, Universitas Airlangga, Surabaya 60115, Indonesia

Abstract Hybridization and electronegativity are fundamental concepts in chemistry connected by Bent's rule. This rule explains many aspects of the structural chemistry and reactivity of organic and inorganic compounds. Over decades, the application of Bent's rule has expanded, demonstrating its wide-ranging utility in elucidating molecular stability due to the substitution of highly electronegative atoms. This study successfully leverages Bent's rule to explain conformational energy difference in acetylcholine case using density-functional calculations. We used butane (Group 2) and butanone (Group 3) families to model the head of ACh^+ and substituted one of the carbons with highly electronegative atoms: B, C, N, and O. This enabled us to evaluate the effects of electronegativity, as well as the presence of carbonyl groups, on their conformational stability and s character. There were three highlighted results. First, our calculations result in the *s* character are consistent with Bent's rule. Second, the high conformational energy differences can be attributed to the changes of *s* character in C2–Z bond: linear in Group 2 and exponential in Group 3, indicating the strong contribution of the carbonyl group. Third, the key determining factor in ACh^+ conformational stability is the carbonyl group, which also strongly contributes to the solute-solvent interactions. Therefore, our study can be further applied to other similar molecules, potentially leading to broader applications in chemistry, especially for understanding ACh^+ stability for Alzheimer's Disease treatment.
Keywords: Acetylcholine, Alzheimer's disease, Bent's rule, Conformational stability, DFT calculations.

Introduction

First introduced by Linus Pauling in 1931[1], hybridization is a fundamental concept in chemistry describing how different atomic orbitals of similar energies combine to form a set of equivalent hybrid orbitals. These hybrid orbitals have different shapes and orientations than the original orbitals, resulting in distinct chemical bond properties [2]. Pauling initially used the hybridization concept to explain the structure of simple molecules such as methane (CH_4). In methane, one 2*s* and three 2*p* orbitals of carbon are hybridized to form four equivalent sp^3 orbitals, each identical in energy. Each sp^3 hybrid orbital then interacts with a 1*s* orbital of a hydrogen atom to form a σ-bond, resulting in four identical covalent C–H σ-bonds [2]. This concept was later applied more widely and is considered an effective heuristic for rationalizing the structures of organic compounds.

A well-established theory by Henry A. Bent in 1960, known as Bent's rule [3-5], is a key link between hybridization and electronegativity. Of three rules, the most widely known is that *s* character tends to concentrate in orbitals toward electropositive substituents, while *p* character tends to concentrate in orbitals toward electronegative substituents. Electronegative substituents refer to the atom with higher electronegativity. Electronegativity is defined as the ability of an atom to attract shared electrons in a covalent bond [2]. It is a crucial property of elements [6], useful in rationalizing the stability [7], structure [8], and properties of molecules [9,10] and solids [11-13]. Therefore, through electronegativity, Bent's rule has successfully linked the hybridization to parameters describing atomic or molecular properties

***For correspondence:**
rusydi@fst.unair.ac.id

Received: 11 June 2024
Accepted: 05 Sept 2024

[14,15], making a great impact on the utility of hybridization-based structural analysis in organic chemistry.

Bent's rule has proven to be a versatile tool in explaining many aspects of the structural chemistry and reactivity of organic and inorganic compounds [14-30]. Over the decades, the application of Bent's rule has expanded, demonstrating its wide-ranging utility. In 1968, William A. Bernet has been successfully explained the unusual chemical reactivity of perfluoroolefins and perfluorocyclopropanes [16]. He discovered that carbon hybrid atomic orbitals in double bonds, carbonyls, and cyclopropyl groups containing a gem-difluoro group are not sp^2 hybridized as formerly thought but are sp^3 hybridized. In 2011, Grabowski reported his two works that utilized Bent's rule to analyze how the hydrogen bond formation influences the positions of bond critical points [20] and to explain the formation of nonbonding interactions [19]. More recently, Zhu *et al*. revealed the importance of Bent's rule in both the thermodynamics and kinetics of the rearrangement of silabenzenes and their monocyclic non-aromatic isomers [21], as well as its role in determining the stability of disilenes and their isomeric silylsilylenes. [24].

Herein, we attempt to leverage Bent's rule in the case of acetylcholine (ACh^+) conformational study. ACh^+ is an organic molecule which associated with the treatment of Alzheimer's Disease due to its role as neurotransmitter in the brain [31]. Based on our previous study [32], ACh^+ possesses seven stable conformers in the gas phase, as shown in Figure 1. These seven stable conformers can be categorized into two groups: low-level energy (tg*g, tgg, ttg, tgt, and ttt) and high-level energy conformers (ctg and ctt) with a discrepancy of about 0.35 eV. They were named by the first three dihedral angles (D), which were D1 (C1–C2–O2–C3), D2 (C2–O2–C4–C5), and D3(O2–C4–C5–N), as shown in Figure 1 (right). The c, g, g*, and t refer to cis, gauche, anticlinal, and trans conformations. For example, the stable conformer in Figure 1 is tg*g, since its dihedral angles of D1, D2, and D3 were trans, anticlinal, and gauche. However, among the eight dihedral angles considered in the previous study, D1 (C1–C2–O2–C4, see Figure 1) significantly determines the order of conformational stability. In our other study [33], when considering the presence of a water solvent, the number of stable ACh^+ conformers was reduced from seven to six, but the role of D1 remained crucial. This fact emphasizes the importance of D1. However, it remains unclear which factors strongly contribute to the conformational stability and solute-solvent interactions of ACh^+: whether it is the presence of the highly electronegative oxygen atom (O2), the carbonyl group attached to C2 (O1), or the other parts of ACh^+.

This paper presents the leverage of Bent's rule to clarify the origin of energy difference between high-level and low-level ACh^+ conformers. The study begins with the selection of simple molecules that vary in the electronegativity of O2 to evaluate its effect. These selected molecules are then optimized using density-functional calculations. The results and discussion are divided into sections covering the validation of the computational method, the electronegativity effect in simple molecules, and the analysis of ACh^+ conformational stability. The impact of water solvent on these conformations is also discussed.

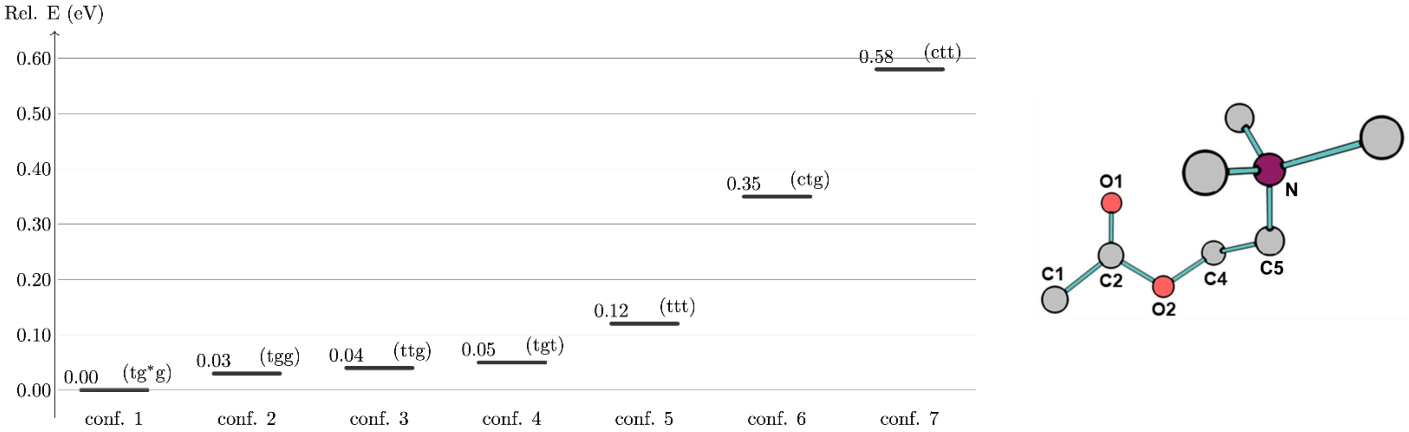

Figure 1. (Left) Energy level diagram (ELD) depicting the seven stable ACh^+ conformers relative to the most stable one. The figure is from [31]. (Right) Illustration of tg*g conformer along with atom numbering

Computational Methods

Conformational Model

Figure 2 shows our molecular models for two families, butane and butanone. We placed Boron (B), Carbon (C), Nitrogen (N), and Oxygen (O) atoms at Z position to raise electronegativity perturbation to the bond of atom 2-3 (the C–Z bond). For the butane family with Z is a C atom, we added two molecules which differed in the sp^n–sp^n of C–Z bond, with n = 1 and 2. Therefore, we had ten unique molecules, as shown in Table 1.

We categorized the butane family into Group 1 (M1, M2, M3) and 2 (M1, M4, M5, M6), while the butanone family as Group 3 (M7, M8, M9, M10). The categorization enabled us to perform comparative analysis, within and between groups, when evaluating the effect of electronegativity and the presence of carbonyl group, C=O.

Figure 2. The computational model of the molecules in this study with the Kekulè structure. The numbers 1 to 4 indicate atom *i*-th, where atom 3 (Z) was replaced by B, C, N, and O atoms with the electronegativity value, in Pauling scale, is 2.04, 2.55, 3.04, 3.44, respectively

Table 1. The list of molecules in this study with the boldface atom refers to "Z" in Figure 2

ID	IUPAC Name	Structure	Formula
M1	Butane	CH_3–CH_2–**C**H_2–CH_3	C_4H_{10}
M2	2-Butene	CH_3–CH=**C**H–CH_3	C_4H_8
M3	2-Butyne	CH_3–C≡**C**–CH_3	C_4H_6
M4	Ethyl(methyl)borane	CH_3–CH_2–**B**H–CH_3	C_3H_9B
M5	N-Methylethylamine	CH_3–CH_2–**N**H–CH_3	C_3H_9N
M6	Methoxyethane	CH_3–CH_2–**O**–CH_3	C_3H_8O
M7	1-(Methylboryl)-1-ethanone	CH_3–CO–**B**H–CH_3	C_3H_7BO
M8	2-Butanone	CH_3–CO–**C**H_2–CH_3	C_4H_8O
M9	N-Methylacetamide	CH_3–CO–**N**H–CH_3	C_3H_7NO
M10	Methyl acetate	CH_3–CO–**O**–CH_3	$C_3H_6O_2$

The torsion angle created by atoms C1–C2–Z–C4 (Figure 2) allows molecular conformation, except for M3. The possible conformation families are staggered and eclipsed. Due to the symmetry of butane and butanone, each family has two possible conformers, as shown in Figure 3. As for M3, the *sp*–*sp* in the C–Z bond forces atoms 1 and 4 to be linear. In this manuscript, both the butane and butanone families used the same torsion angle (C1–C2–Z–C4) to define the conformers.

Ground State Optimization

We utilized DFT [34], [35] for determining the ground electronic state of these molecules in the gas phase. We followed the optimization routine as we have described in our previous study [36]. In this study, we used B3LYP/6-311++G(d,p) as the exchange-correlation functional/basis set integrated into Gaussian 16 software [37]. We ran the vibrational modes calculations to ensure no imaginary frequency in the optimized structures and correct the electronic energy from the DFT calculations with thermal energy. The vibrational modes calculations were at room temperature and without any scale factor applied. Additionally, we performed Natural Bond Orbital (NBO) calculations using NBO 3.1 [38]. These NBO calculations provide a detailed picture of the bonding and electronic interactions in a molecule by transforming the wave function from a delocalized molecular orbital (MO) basis to a localized natural bond orbital basis.

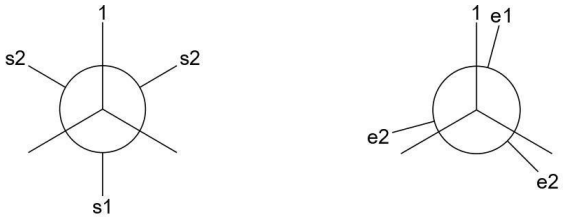

(a) staggered (b) eclipsed

Figure 3. The four possible conformers of molecules in Figure 1 in Newman projections. Atom 4 in s1 position is *trans* (t), in s2 is *gauche* (g), and in e1 is *cis* (c)

Computation With Water Solvent

We employed Polarizable Continuum Model (PCM) [39] to study the conformer's structure in the presence of water solvent. The change in the electronic energy upon the introduction of water solvent indicates their water solubility: the more stable the conformer, the more soluble it is. The solvent may affect the optimized geometry as well; therefore, we examined the change of C–Z bond length, and, more importantly, its dipole moment in the presence of water solvent. Since PCM treats the solvent as a charged cavity with a specific dielectric constant, the change in the molecule's dipole moment represents the change in the molecule's charge distribution due to the electrostatic field from the cavity. Therefore, the larger the dipole moment changes, the stronger the interaction between the molecule and the solvent.

Computation Model Assessment

We systematically assessed our computational model through comparison with established knowledge and experimental results. First, we confirmed that the ground spin state of molecules in Group 1 were singlet, which has been well-known. Second, we compared our calculations results to the experimentally observed geometrical parameters. Third, we ensure our result aligns with Bent's rule prior to perform further analysis on geometry, bond orbital, and electronegativity. According to Bent's rule [4], [5], if Z is substituted by atom with higher electronegativity, s character at C2 tends to concentrate in orbitals toward electropositive group, C1. Therefore, C1–C2 bond becomes shorter. To apply Bent's rule, we compared s character at C2 (C2–C1 bond) in each group, both in the gas phase and water solvent. In addition, we ensured that our calculation results lie within acceptable accuracy of B3LYP/6-311++G(d,p), which has an RMS error of 1.4° for the angle and 0.017 Å for the bond length [40].

Results and Discussion

We divided this section into three parts. The first part discusses the computational method goodness based on electronic and thermal energy, geometrical structure, water solubility, and *s* character. The second part evaluates the effect of electronegativity on the conformational stability and *s* character in the absence and presence of carbonyl group. The last part was to escalate our analysis from the simple molecule model to acetylcholine (ACh^+) conformers.

The Computational Method Goodness

Electronic and thermal energy. The geometry optimization of Group 1 (M1, M2, and M3 in Table 1) determined that their ground singlet state is lower in energy than their ground triplet state. Figure 4 shows their stability in an energy level diagram. The energy difference between singlet and triplet states was significantly large, about 2.60 eV and 3.60 eV for M2 and M3, respectively. For M1, the optimization of its triplet state broke the molecule up, which indicates that butane is unstable in its triplet state.

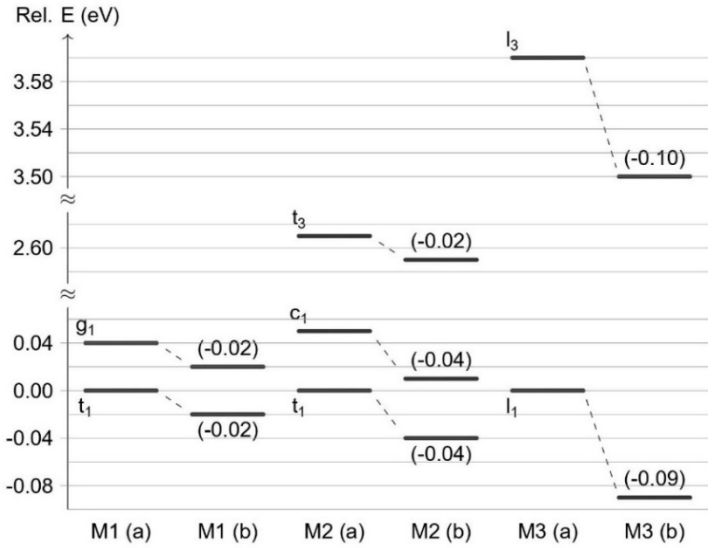

Figure 4. The energy level diagram of Group 1 in (a) the gas phase and (b) the water solvent. The symbols t, g, and c refer to Figure 3 with addition "l" for linear. The index 1 and 3 are for singlet and triplet spin states. The numbers in parentheses are the energy difference between (b) and (a)

In their singlet state, M1 and M2 exist as two stable conformers. Both M1 and M2 are well known to have two conformers, trans and gauche, with the former being more stable than the latter due to the repulsion between the bulky group at C1 and C4. The calculations confirmed that the trans conformer is consistently lower in energy.

DFT calculations predicted that all molecules in Groups 2 and 3 have two stable conformers, except for M7, as shown in Figures 5 and 6. Those two stable conformers were either trans and cis or trans and gauche, while M7 only had gauche conformation. Figures 4 and 5 show that trans was the most stable conformer for all molecules in the groups.This result is consistent with experimental observations for M1 [41], M6 [42], M8 [43], M9 [44], and M10 [45].

Table 2 shows the thermal energy difference between the conformers with available experimental data available. It was the same quantity with the energy difference in Figure 4 (for all molecules and conformers), but the former contained the thermal correction from the vibrational mode calculations. While the standard Gibbs free energy calculation for M1 falls outside of the experimental error range, the overall calculated trend is comparable with the general experimental trend. Applying the scale factor to the vibrational mode calculations can improve the accuracy, as demonstrated by [46]. It implies that B3LYP/6-311++G(d,p) is reasonable for the energetic study of butane and butanone families.

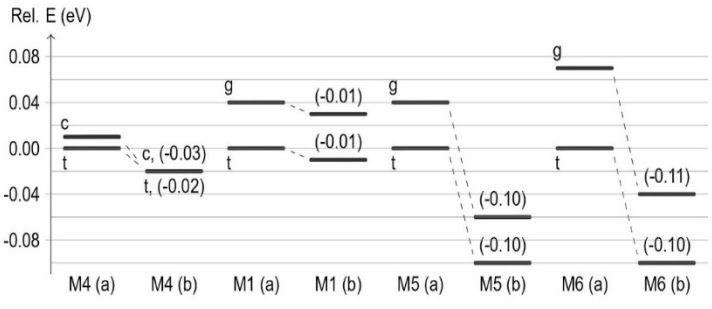

(a) Group 2

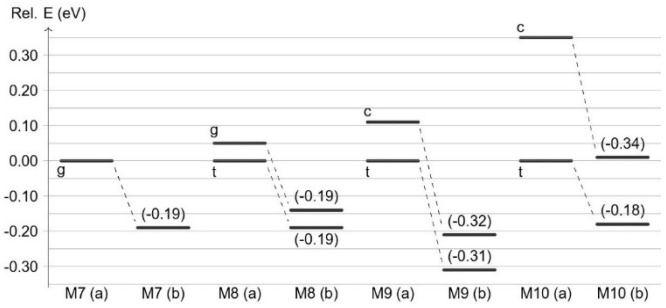

(b) Group 3

Figure 5. The energy level diagrams for Group 1 and 2 in (a) the gas phase and (b) the water solvent. The symbols t, g, and c refer to Figure 3. The numbers in parentheses are the energy difference between (b) and (a)

Table 2. The comparison of thermal energy difference between two conformers (cal/mol) from experimental data (Expr.) and this study (Calc.) in form of the standard enthalpy (ΔH°) or in the standard Gibbs free energy (ΔG°)

Molecule	Energy	Expr.			Calc.	Δ (Expr. - Calc.)
		Mean	Error	Refr.		
M1	ΔG°	497	±220	[41]	902	425
M2	ΔH°	1,043	±196	[47]	1,153	110
M6	ΔG°	1,230	±270	[42]	1,384	154
M8	ΔG°	2,100	±400	[43]	1,614	-486
M9	ΔH°	2,300	n.r.	[48]	2,537	237
M10	ΔH°	8,500	±1,000	[49]	7,841	-659

Table 3. Geometric parameters for the bond length (*R*) in Å, the torsion angle (θ) in degree (°), and dipole moment (μ) in debye

Molecule	R_1(C1–C2)*		R_1(C1–C2)		R_2(C2–Z)*	R_2(C2–Z)		*θ*		μ	
	[Ref.]	(a) (rms)	(a)	(b)	(a) (rms)	(a)	(b)	(a)	(b)	(a)	(b)
Group 1											
M1-t	[41]	1.531 (2)	1.531	1.532	1.531(2)	1.533	1.533	180.0	180.0	0.0	0.0
M1-g	[41]	1.531(2)	1.533	1.533	1.531(2)	1.537	1.537	65.6	65.9	0.1	0.1
M2-t	[50]	1.508(2)	1.501	1.502	1.347(3)	1.333	1.334	180.0	180.0	0.0	0.0
M2-c	[50]	1.506(2)	1.502	1.503	1.346(3)	1.336	1.338	0.0	0.0	0.3	0.4
M3-l	[51]	1.467(13)	1.459	1.461	1.213(13)	1.204	1.206	1.2	2.1	0.0	0.0
Group 2											
M4-t	n.a.	-	1.536	1.536	-	1.565	1.564	162.6	162.8	0.5	0.6
M4-c	n.a.	-	1.535	1.535	-	1.567	1.566	0.4	0.4	0.3	0.4
M5-t	n.a.	-	1.525	1.525	-	1.461	1.466	178.6	177.7	1.0	1.5
M5-g	n.a.	-	1.529	1.528	-	1.465	1.469	75.4	75.7	1.0	1.5
M6-t	[42]	1.520(4)	1.517	1.517	1.418(2)	1.420	1.427	180.0	180.0	1.3	1.8
M6-g	[42]	1.520(4)	1.527	1.525	1.418(2)	1.423	1.430	75.1	75.0	1.5	2.0
Group 3											
M7-g	n.a.	-	1.505	1.502	-	1.573	1.578	180.0	180.0	3.0	4.2
M8-t	[43]	1.518	1.518	1.512	1.518	1.523	1.517	75.1	75.0	3.0	4.1
M8-g	[43]	1.518	1.516	1.510	1.518	1.523	1.517	92.8	89.9	3.1	4.2
M9-t	[44]	1.520(5)	1.519	1.515	1.386(4)	1.368	1.351	174.0	173.5	3.9	5.4
M9-c	n.a.	-	1.518	1.514	-	1.370	1.354	89.9	87.3	4.3	5.8
M10-t	[45]	1.496(6)	1.507	1.504	1.360(6)	1.352	1.345	180.0	180.0	1.9	2.5
M10-c	n.a.	-	1.515	1.350	-	1.362	1.350	6.1	1.2	4.8	6.3

Note: (*) for experimental data

Geometrical structure. The DFT calculations obtained the geometry of Group 1 and other well-known molecules in Group 2 and 3 with acceptable accuracy. These other well-known molecules were M6, M8, M9, and M10. The acceptable accuracy is implicitly shown in Table 3. Table 3 shows that the calculated bond lengths of all molecules, R_1 and R_2, were very close to the experimental data, with discrepancies less than 0.017 Å (see "*Computational model assessment*" in "*Computational Method*" section). Table 3 also shows that the torsional angle, *θ*, of M1-g was also close to the experimental data, with discrepancies less than 1.4°. Meanwhile, for M6-g and M8-g, their experimental values were 86±6° [41] and 70° (assumed during the measurement) [45]. The differences with the calculations were larger than 1.4°. However, the experimental and computational results agree that the gauche structures of M6 and M8 are in the synclinal region of the Newman projection.

Water solubility. The DFT coupled with PCM calculations predicted the water solubility of some molecules in Group 2 and 3 with good accuracy. We may infer their water solubility from the change of energy level and dipole moments in the presence of water solvent. Except for M4 and M5, their energy difference in the presence and absence of water was larger than 0.1 eV (Figure 5). Their dipole moment also changed by more than 0.5 debye (see Table 3). The changes in Group 3 are larger than in Group 2. It implies that the presence of water significantly changes their structures. Therefore, PCM predicted not only attractive interactions between the molecule and water solvent, but also the water solubility of the butanone family is higher than that of the butane family. These predictions agree with experimental data for M6, M7, M8, M9, and M10 [52]. Consequently, M4-t, M4-c, M5-t, and M5-g should be insoluble in the water solvent.

***s* character.** DFT coupled with NBO calculations also predicted *s* character with a good accuracy. Figure 6 shows a linear dependence of *s* character of C2 in C2–Z bond to the bond order of C2–Z from Group 1. The figure shows that the higher the number of bond order, the higher the allocated *s* character in the σ bond, which is theoretically correct [2].

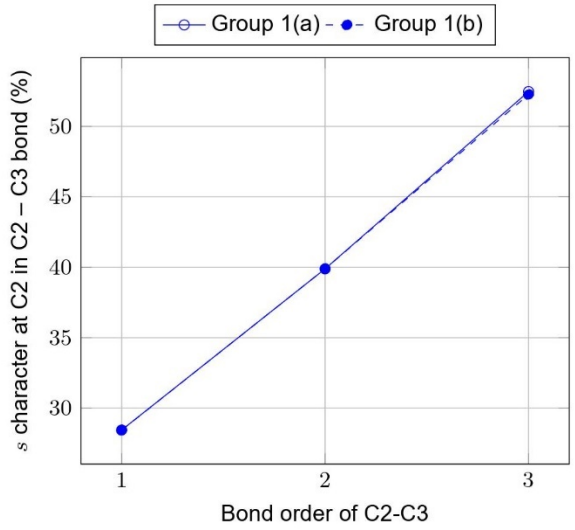

Figure 6. The *s* character (%) of (a) C2 in C2-C3 vs bond order of C2-C3 in molecules from Group 1, which are M1 (single), M2 (double), and M3 (triple)

The Effect of Electronegativity

Effect on the conformational stability. The change in electronegativity of the Z atom affects the conformational stability of all molecules in Groups 2 and 3, as depicted in Figures 5 and 7. These figures illustrate the electronegativity effect in two different ways: an energy level diagram (ELD) for the change in electronic energy (eV) and a plot of conformational energy differences (ΔE) versus the electronegativity of the Z atom.

The most significant effect in each group occurred when Z was substituted by oxygen: M6 (Group 2) and M10 (Group 3), as shown in Figure 5. Their conformational energy differences were 0.7 and 0.35 eV, respectively—up to seven times higher than those of M4 and M8. This significant effect can be attributed to the high electronegativity of oxygen, which is the highest among the elements B, C, N, and O. Generally, the higher the electronegativity at the Z position, the higher the conformational energy difference.

Figure 7 shows the relationship between the electronegativity of the Z atom and ΔE for all groups. This relationship is linear in Group 2 and exponential in Group 3, indicating that the conformational stability of molecules in the presence of a carbonyl group (Group 3) is more sensitive to electronegativity changes than in Group 2. This sensitivity is further emphasized by the conformational energy difference between M6 (Group 2) and M10 (Group 3), where the conformational energy difference in M10 is approximately five times higher.

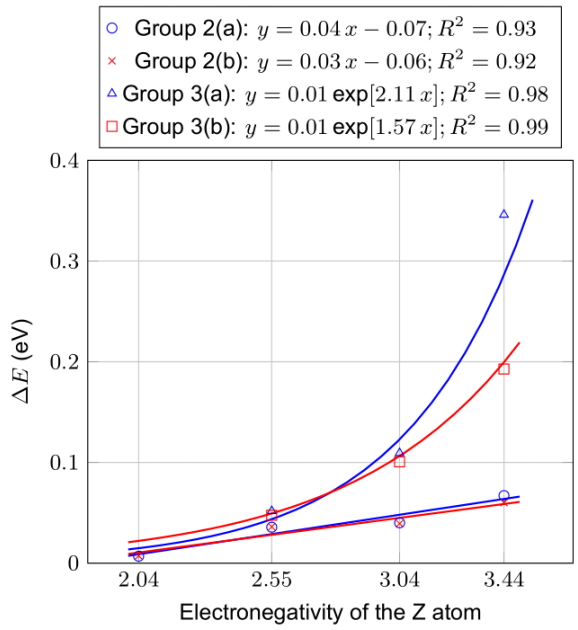

Figure 7. The conformational energy differences in term of electronic energy (eV) in Groups 2 and 3 versus the electronegativity of the Z atom both in the gas phase (a) and water solvent (b) together with their fitting functions

Effect on the *s* character. The change in electronegativity of the Z atom affects the s character of C2 (in C1–C2 and C2–Z) and of C4 (in C4–H), as depicted in Figures 8(a)-(c). Figures 8(a) and 8(c) show that increasing the electronegativity of the Z atom increases the percentage of s character at the C atoms (C2 and C4). Meanwhile, Figure 8(b) shows the opposite trend. These results imply that our calculations, presented in Figure 8, are consistent with Bent's rule [4], [5]: the increase in electronegativity causes the s character to be more concentrated in orbitals directed towards the electropositive groups (C1–C2 and C4–H), and consequently, the p character is directed towards the electronegative groups. Furthermore, our results agree with other computational studies [20], [23].

Despite the different trends, Figures 8(a) and 8(b) both show that C2 (in both C1–C2 and C2–Z) in Group 3 possesses more s-character than in Group 2. Specifically, C2 in Group 3 has up to 6.6% more *s* character in C1–C2 and 7.9% more in C2–Z. These results further confirm the role of the carbonyl group (exist in Group 3) in the aforementioned discussions (effect on conformational stability). Meanwhile, in Figure 8(c), C4 (in C4–H) in Groups 2 and 3 possess a similar percentage of *s* character, indicating that electronegativity primarily affects the hybridization in C1–C2 and C2–Z bonds, as stated in Bent's rule.

We plotted the conformational energy difference against *s* character at C2 in C2–C1 and C2–Z bonds in Figure 9(a) and (b). Figure 9(a) shows that hybridization in C2-C1 bond possesses linear trend for all groups with Group 3 having higher gradient value—up to four times. Meanwhile, in Figure 9(b), we found out that hybridization in C2–Z has similar trend to the one in Figure 7: linear in Group 2 and exponential in Group 3. Both Figures 9(a) and (b) indicate that the conformational energy differences of M1, and M4-M10 are more sensitive to the changes of *s* character in Group 3 than in Group 2, especially in the case of C2–Z bond. This fact highlights the contribution of carbonyl group in the changes of *s* character, or bond hybridization, as well as the conformational stability of molecules.

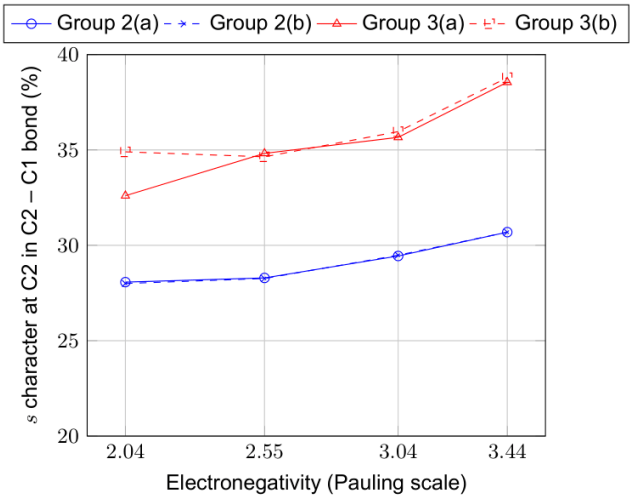

(a) *s* character at C2 in C2–C1

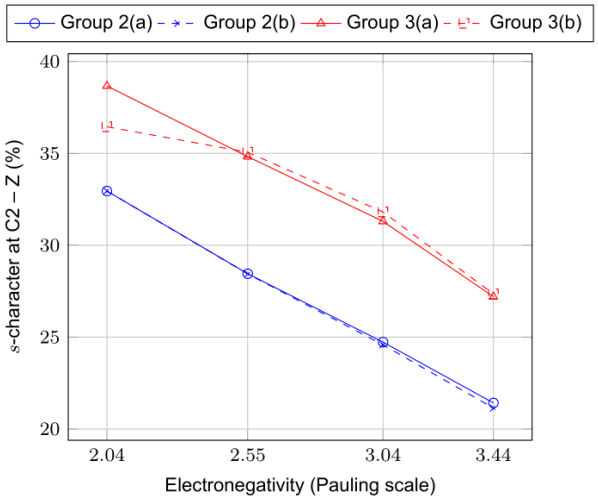

(b) *s* character at C2 in C2–Z

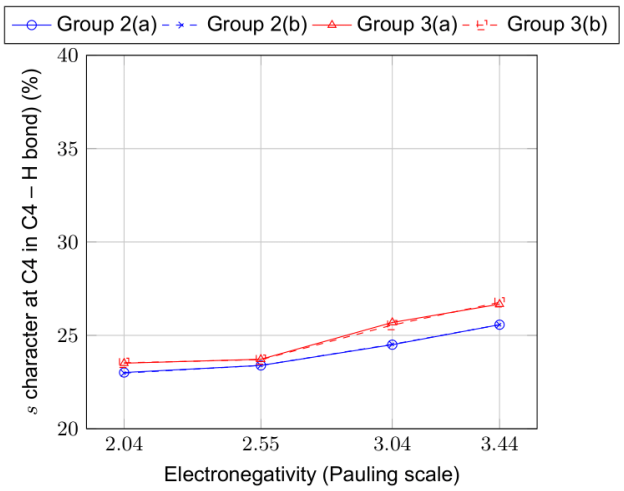

(c) *s* character at C4 in C4–H

Figure 8. The *s* character (%) at C2 in (a) C2–C1 and C2–Z bond, and (c) C4 in C4–H bond vs electronegativity of Z atom from Groups 2 and 3 in the gas phase (a) and water solvent (b)

We also reveal that Groups 2 and 3 show a more significant change in the percentage of *s* character when the substituent changes from N to O, compared to B to C (see Figure 8). Additionally, O consistently shows the highest percentage of *s* character, which aligns with the discussion on the electronegativity effects on conformational stability. Since O has a high electronegativity, it pulls electron density towards itself more strongly than the less electronegative atoms, causing drastic changes in the distribution of s and p characters in hybrid orbitals. This result underscores the potential of the rehybridization effect, which may increase for more electronegative substituents [23].

Effect of water solvent. The presence of water solvent significantly affects the conformational stability in M10 and *s* character in M7 as shown in Figure 5. Except for M10, the changes in conformational energy difference after the presence of water solvent were around 0.01 eV. Meanwhile, for M10, the change in energy was 0.16 eV—up to sixteen times higher than others.

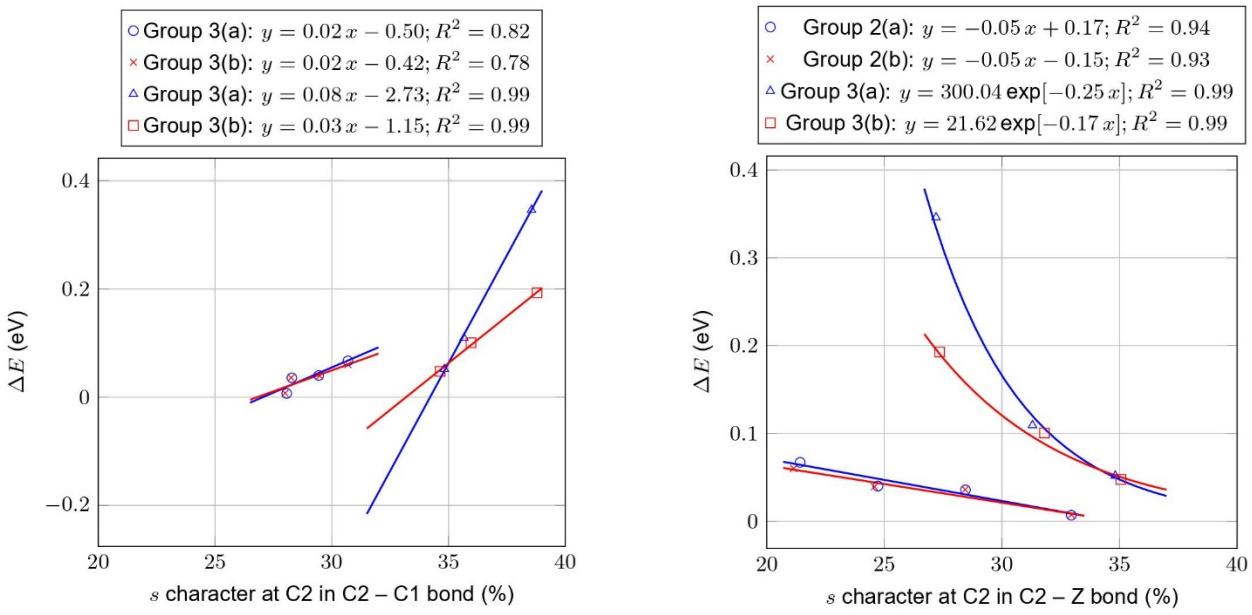

(a) at C2 in C1–C2 bond (b) at C2 in C2–Z

Figure 9. The conformational energy differences in term of electronic energy (eV) in Groups 2 and 3 versus the *s* character (%) at C2 in (a) C1–C2 and (b) C2–Z both in the (a) gas phase and (b) water solvent together with their fitting functions

The Stability of Acetylcholine (ACh^+) Conformers

The conformational energy difference between the high- and low-energy conformers of M10 is similar to that of ACh^+ in a previous study [32] as shown in Table 4. In the gas phase, the conformational energy difference of M10 (t and c) is 0.35 eV, while for ACh^+ (ttg and ctg), it is 0.32 eV. The discrepancy is only 0.03 eV, which is very small. Since M10 is analogous to D1 (C1–C2–O2–C4 of ACh^+), it can be concluded that D1 is a key determinant of the overall conformational stability of ACh^+. Our previous discussion about s character confirms the role of D1 (constructed by atoms C1–C2–O2–C4) at the head of ACh^+ in determining the energy difference between its low- and high-energy conformers. In addition to ACh^+, M10 is also analogous to θ_4 and θ_7 of curcumin, which we investigated recently [53]. This result confirms the importance of considering M10-like structures when constructing possible conformers of molecules.

This similar trend also occurred in the presence of water solvent. The conformational energy difference of M10 was very close to that of ACh^+ as shown in Table 4. According to our previous discussion, carbonyl group is the one who responsible in the energy decreased. It implies that D1 is not only significant in the gas phase, but also in the water solvent. Therefore, D1 is the one that strongly contributes on the solute-solvent interactions of ACh^+.

Table 4. The list of conformational energy differences (in eV) of ACh^+ and M10

No.	Environment	Conformational energy difference (ΔE) in eV	
		ACh^+ (ttg - ctg)	M10 (t - c)
1.	Gas phase	0.32	0.35
2.	Water solvent	0.19	0.21

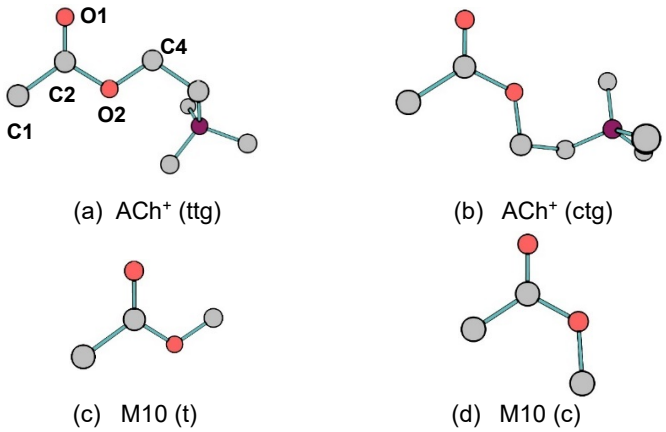

Figure 10. Geometrical structure of acetylcholine (ACh^+) with dihedral angle, D1, consist of C1–C2–O2–C4 and methyl acetate (M10) conformers. For clarity, all of hydrogen atoms are not displayed

Conclusion

We successfully demonstrated the applicability of Bent's rule in the case of acetylcholine (ACh^+) conformational study using a first-principles framework. By substituting one carbon atom with highly electronegative atom (C2–Z bond, with Z = B, C, N, and O) in the butane (Group 2) and butanone (Group 3) families, we can evaluate the influence of electronegativity of the Z atom (hybridized bond type C2–Z) and the presence of carbonyl group in their conformational stability. We revealed the difference relationship of conformational energy difference (ΔE) and electronegativity of the Z atom: linear in Group 2 and exponential in Group 3. This result highlights the importance of oxygen atom in hybridized bond type C2–Z and its strong contribution in carbonyl group.

Our calculation results on the *s* character of C2–Z, C2–C1, and C4–H bonds shows a good alignment with Bent's rule. According to our Bent's rule analysis, the significant difference in the conformational energy (ΔE) can be attributed to the changes in the *s* character of the C2–Z bond, which parallels the trend in electronegativity. This underscores the importance of the carbonyl group's presence. This trend appears in ACh^+, which has similar geometrical structure with group 3. It confirms the role of D1 (constructed by atom C1–C2–O2–C4) at the head of ACh^+ in determining the energy difference between its low- and high-level conformers and on the solute-solvent interactions. Additionally, that relation between ΔE and the changes of *s* character could be used to explain the different conformational stability in curcumin structure, according to our previous study. Therefore, these results have proven the extent of Bent's rule and its applicability in this fundamental chemical theory. Our study can be further applied to other similar molecules, potentially leading to broader applications in chemistry.

Conflicts of Interest

The authors declare that there is no conflict of interest regarding the publication of this paper.

Acknowledgement

This study was supported by Lembaga Penelitian dan Pengabdian Masyarakat Universitas Airlangga through "Hibah Riset Mandat Top Tier 2021" with grant number 769/UN3.15/PT/2021. All calculations using Gaussian 16 software were carried out in the computational facility "Riven" at the Research Center for Quantum Engineering Design, Universitas Airlangga, Indonesia. Author thanks Prof. Yoshitada Morikawa *and Rizka N. Fadilla* (Graduate School of Engineering, Osaka University, Japan), Prof. Darminto (Physics, Institut Teknologi Surabaya, Indonesia), *and Roichatul Madinah (Chemistry, Universiti Kebangsaan Malaysia, Malaysia)* for valuable discussion and support.

References

[1] Pauling, L. (1931). The Nature of the Chemical Bond. Application of Results Obtained from The Quantum Mechanics and From a Theory of Paramagnetic Susceptibility to the Structure of Molecules. *Journal of American Chemical Society*, *53*, 1367–1400.

[2] McMurry, J. (2015). *Organic chemistry* (9th ed.). USA: Cengage Learning.

[3] Bent, H. A. (1960). Electronegativities from Comparison of Bond Lengths in AH and AH^+. *The Journal of Chemical Physics*, *33*(4), 1258–1259.

[4] Bent, H. A. (1960). Correlation of Bond Shortening by Electronegative Substituents with Orbital Hybridization. *The Journal of Chemical Physics*, *33*(4), 1259–1260.

[5] Bent, H. A. (1960). Bond Shortening by Electronegative Substituents. *The Journal of Chemical Physics*, *33*(4), 1260–1261.

[6] Tantardini, C., & Oganov, A. R. (2021). Thermochemical electronegativities of the elements. *Nature Communications*, *12*(1), 2087.

[7] Szatyłowicz, H., & Krygowski, T. M. (2007). Varying electronegativity: Effect of the Nature and Strength of H-bonding in Anilide/Aniline/Anilinium Complexes on the Electronegativity of $NH=NH_2=NH_3^+$ groups. *Journal of Molecular Structure*, *844–845*, 200–207.

[8] Campanelli, A. R., Domenicano, A., & Ramondo, F. (2003). Electronegativity, Resonance, and Steric Effects and the Structure of Monosubstituted Benzene Rings: An ab Initio MO Study. *The Journal of Physical Chemistry A*, *107*(33), 6429–6440.

[9] Wetmore, S. D., Schofield, R., Smith, D. M., & Radom, L. (2001). A Theoretical Investigation of the Effects of Electronegative Substitution on the Strength of C−H···N Hydrogen Bonds. *The Journal of Physical Chemistry A*, *105*(38), 8718–8726.

[10] Appleton, A. L., Brombosz, S. M., Barlow, S., Sears, J. S., Bredas, J. L., Marder, S. R., & Bunz, U. H. F. (2010). Effects of Electronegative Substitution on the Optical and Electronic Properties of Acenes and Diazaacenes. *Nature Communications*, *1*, 91.

[11] Lu, J., Jin, H., Dai, Y., Yang, K., & Huang, B. (2012). Effect of Electronegativity and Charge Balance on the Visible-Light-Responsive Photocatalytic Activity of Nonmetal Doped Anatase TiO_2. *International Journal of Photoenergy*, 928503.

[12] Chen, H., Yang, M., Liu, J., Lu, G., & Feng, X. (2020). Insight into effect of electronegativity on H2 catalytic activation for CO2 hydrogenation: Four transition metal cases from a DFT study. *Catalysis Science & Technology*, *10*(16), 5641–5647.

[13] Chen, H., Fu, W., Geng, Z., Zeng, J., & Yang, B. (2021). Inductive Effect as a Universal concept to design efficient catalysts for CO2 electrochemical reduction: electronegativity difference makes a difference. *Journal of Materials Chemistry A*, *9*(8), 4626–4647.

[14] Alabugin, I. V., & Manoharan, M. (2007). Rehybridization as a general mechanism for maximizing chemical and supramolecular bonding and a driving force for chemical reactions. *Journal of Computational Chemistry*, *28*(1), 373–390.

[15] Alabugin, I. V., Manoharan, M., Peabody, S., & Weinhold, F. (2003). Electronic Basis of Improper Hydrogen Bonding: A Subtle Balance of Hyperconjugation and Rehybridization. *Journal of American Chemical Society*, 125(19), 5973–5987.

[16] Bernett, W. A. (1968). Hybridization Effects in Fluorocarbons. *The Journal of Organic Chemistry*, *34*(6), 1772–1776.

[17] Alabugin, I. V., Manoharan, M., Buck, M., & Clark, R. J. (2007). Substituted anilines: The tug-of-war between pyramidalization and resonance inside and outside of crystal cavities. *Journal of Molecular Structure*: *Theochem*, *813*(1–3), 21–27.

[18] Kandemirli, F., Hoscan, M., Dimoglo, A., & Esen, S. (2008). Theoretical Study and Comparison of Bent's Rule with Hardness and Polarizability for SF_4, SF_4O, PCl_4F, PCl_3F_2, PCl_2F_3, PCl_2F_4 Molecules. *Phosphorus, Sulfur, and Silicon and the Related Elements*, *183*(8), 1954–1967.

[19] Grabowski, S. J. (2011). Red- and Blue-Shifted Hydrogen Bonds: the Bent Rule from Quantum Theory of Atoms in Molecules Perspective. *The Journal of Physical Chemistry A*, *115*(44), 12340–12347.

[20] Grabowski, S. J. (2011). Theoretical study on the interconversion of silabenzenes and their monocyclic non-aromatic isomers via the [1,3]-substituent shift: Interplay of aromaticity and Bent's rule. *The Journal of Physical Chemistry A*, *115*(45), 12789–12799.

[21] Wang, X., Huang, Y., An, K., Fan, J., & Zhu, J. (2014). Theoretical study on the interconversion of silabenzenes and their monocyclic non-aromatic isomers via the [1,3]-substituent shift: Interplay of aromaticity and Bent's rule. *Journal of Organometallic Chemistry*, *770*, 146–150.

[22] Medina, J. M., Mackey, J. L., Garg, N. K., & Houk, K. N. (2014). The Role of Aryne Distortions, Steric Effects, and Charges in Regioselectivities of Aryne Reactions. *Journal of The American Chemical Society*, *136*(44), 15798–15805.

[23] Alabugin, I. V., Bresch, S., & Manoharan, M. (2014). Hybridization Trends for Main Group Elements and Expanding the Bent's Rule Beyond Carbon: More than Electronegativity. *The Journal of Physical Chemistry A*, *118*(20), 3663–3677.

[24] Huang, Y., Wu, J., Qiu, R., Xu, F., & Zhu, J. (2020). Probing the Tautomerization of Disilenes and Disilabenzenes with Their Isomeric Silylenes: Significant Substituent, Aromaticity and Base Effects. *Dalton Transactions*, *49*(47), 17341–17349.

[25] Kang, D., Cheung, S. T., & Kim, J. (2021). Bioorthogonal Hydroamination of Push-Pull-Activated Linear Alkynes. *Angewandte Chemie International Edition*, *60*(31), 16947–16952.

[26] Zhou, W., Pan, W., Chen, J., Zhang, M., Lin, J., Cao, W., & Xiao, J. (2021). Transition-metal difluorocarbene complexes. *Chemical Communications*, *57*(74), 9316–9329.

[27] Izod, K., Madlool, A. M., Craig, A., & Waddell, P. G. (2022). Substituent Effects on the Structures of Alkali Metal Phosphido-Borane Complexes. *European Journal of Inorganic Chemistry*, *2022*(15), E202200123.

[28] Karandikar, S. S., Bhattacharjee, A., Metze, B. E., Javaly, N., Valente, E. J., McCormick, T. M., & Stuart, D. R. (2022). Orbital Analysis of Bonding in Diarylhalonium Salts and Relevance to Periodic Trends in structure and Reactivity. *Chemical Science*, *13*(22), 6352–6540.

[29] Pinhas, A. R., Kugel, R. W., & Jensen, W. B. (2024). Elaborating the Link Between VSEPR and Orbital Hybridization. *International Journal of Chemistry*, *16*(1), 57.

[30] Paul, B. K. (2024). Blue- and Red-Shifting C−H···O Hydrogen Bonds of Cyclic Ethers with Haloforms: Effect of Ring-Size and Consistency with Bent's Rule. *ChemPhysChem*, E202400263.

[31] Gauthier, S. (2002). Advances in the pharmacotherapy of Alzheimer's disease. *Canadian Medical Association Journal*, *166*(5), 616–623.

[32] Fadilla, R. N., Rusydi, F., Aisyah, N. D., Khoirunisa, V., Dipojono, H. K., Ahmad, F., Mudasir, & Puspitasari, I. (2020). A Density-functional Study of the Conformational Preference of Acetylcholine in the Neutral Hydrolysis. *Molecules*, *25*, 670.

[33] Fadilla, R. N., Rusydi, F., Madinah, R., Dipojono, H. K., Ahmad, F., Mudasir, Puspitasari, I., & Morikawa, Y. (2023). Acetylcholine Conformational Flexibility and Its Neutral Hydrolysis in Aqueous Solution. *ChemistrySelect*, *8*(15), 1–15.

[34] Kohn, W., & Sham, L. J. (1965). Self-Consistent Equations Including Exchange and Correlation Effects. *Physical Review A*, *140*(4A), A1133.

[35] Hohenberg, P., & Kohn, W. (1964). Inhomogeneous Electron Gas. *Physical Review*, *136*(3B), B864.

[36] Rusydi, F., Madinah, R., Puspitasari, I., Fui, M. L. W., Ahmad, A., & Rusydi, A. (2021). Teaching Reaction Kinetics through Isomerization Cases with the Basis of Density-functional Calculations. *Biochemistry and Molecular Biology Education*, 49(2), 216–227.

[37] Frisch, M. J., *et al.* (2016). Gaussian 16 Revision C.01.

[38] Glendening, E. D., Landis, C. R., & Weinhold, F. (2013). Natural bond orbital analysis program. *Journal of Computational Chemistry*, *34*(16), 1429–1437.

[39] Tomasi, J., Mennucci, B., & Cammi, R. (2005). Quantum mechanical continuum solvation models. *Chemical Reviews*, *105*(8), 2999–3093.

[40] Young, D. C. (2001). *Computational chemistry: A practical guide for applying techniques to real world problems.* John Wiley & Sons.

[41] Bradford, W. F., Fitzwater, S., & Bartell, L. S. (1977). Molecular Structure of n-Butane: Calculation of Vibrational Shrinkages and an Electron Diffraction Reinvestigation. *Journal of Molecular Structure*, *38*, 185–194.

[42] Oyanagi, K., & Kuchitsu, K. (1978). Molecular Structure and Conformation of Ethyl Methyl Ether as Studied by Gas Electron Diffraction. *Bulletin of the Chemical Society of Japan*, *51*(8), 2237–2242.

[43] Abe, M., Kuchitsu, K., & Shimanouchi, A. T. (1969). Electron-Diffraction Study of Rotational Isomerism of Methyl Ethyl Ketone. *Journal of Molecular Structure*, *4*, 245–253.

[44] Kitano, M., Fukuyama, T., & Kuchitsu, K. (1973). Molecular Structure of *N*-Metyhlacetamide as Studied by Gas Electron Diffraction. *Bulletin of the Chemical Society of Japan*, *46*, 384–387.

[45] Pyckhout, W., Van Alsenoy, C., & Geise, H. J. (1986). Structure of Gaseous Methyl Acetate as Determined by Joint Analysis of Electron Diffraction, Microwave and Infrared Spectroscopy, Supplemented by a Valence Force Field and Constraints from Geometry Relaxed Ab Initio Calculations. *Journal of Molecular Structure*, *144*, 265–279.

[46] Kang, Y. K. (2001). Ab Initio MO and Density Functional Studies on Trans and Cis Conformers of N-Methylacetamide. *Journal of Molecular Structure*: *Theochem*, *546*, 183–193.

[47] Prosen, E. J., & Rossini, F. D. (1946). Heats of Formation, Hydrogenation, and Combus-Tion of The Monoolefin Hydrocarbons Through the Hexenes, and of the Higher l-Alkenes, in the Gaseous State at 25°C. *Journal of Research of the National Bureau of Standards*, *36*.

[48] Ataka, S., Takeuchi, H., & Tasuni, M. (1984). Infrared Studies of the Less Stable Cis Form of N-Methylformamide and N-Methylacetamide in Low-temperature Nitrogen Matrices and Vibrational Analyses of the Trans and Cis Forms of These Molecules. *Journal of Molecular Structure*, *113*, 147–160.

[49] Blom, C. E., & Gunthard, H. H. (1981). Rotational Isomerism in Methyl Formate and Methyl Acetate; a Low-Temperature Matrix Infrared Study Using Thermal Molecular Beams. *Chemical Physics Letters*, *84*(2).

[50] Almenningen, A., Anfinsen, I. M., & Haaland, A. (1970). Electron Diffraction Studies of cis- and trans-2-Butene. *Acta Chemica Scandinavica*, *24*, 43–49.

[51] Tanimoto, M., Kuchitsu, K., & Morino, Y. (1969). Bond Length of Dimethylacetylene as Determined by Gas Electron Diffraction. *Bulletin of the Chemical Society of Japan*, *42*, 2519–2523.

[52] Haynes, W. M., Lide, D. R., & Bruno, T. J. (2017). *CRC handbook of chemistry and physics* (97th ed.). CRC Press.

[53] Madinah, R., Rusydi, F., Fadilla, R. N., Khoirunisa, V., Boli, L. S. P., Saputro, A. G., Hassan, N. H., & Ahmad, A. (2023). First-Principles Study of the Dispersion Effects in the Structures and Keto-Enol Tautomerization of Curcumin. *ACS Omega*, *8*(37), 34022–34033.